

## Excitation energy deposition in $^{209}\text{Bi}(\alpha, \alpha')$ reactions at 240 MeV

D. Fabris,<sup>1</sup> M. Lunardon,<sup>1</sup> G. Nebbia,<sup>1</sup> G. Viesti,<sup>1</sup> M. Cinausero,<sup>2</sup> E. Fioreto,<sup>2</sup> D. R. Napoli,<sup>2</sup> G. Prete,<sup>2</sup> K. Hagel,<sup>3</sup> J. B. Natowitz,<sup>3</sup> R. Wada,<sup>3</sup> P. Gonthier,<sup>3,\*</sup> Z. Majka,<sup>3,†</sup> R. Alfaro,<sup>3,‡</sup> Y. Zhao,<sup>3</sup> N. Mdeiwayah,<sup>3</sup> and T. Ho<sup>3</sup>

<sup>1</sup>*I.N.F.N. and Dipartimento di Fisica dell' Università di Padova, I-35131 Padova, Italy*

<sup>2</sup>*I.N.F.N., Laboratori Nazionali di Legnaro, I-35020 Legnaro, Italy*

<sup>3</sup>*Cyclotron Institute, Texas A&M University, College Station, Texas 77843*

(Received 13 January 1998)

The energy deposition associated with inelastic  $\alpha$  particle scattering on  $^{209}\text{Bi}$  at 240 MeV has been determined using the TAMU neutron ball. A comparison of the reconstructed average excitation energies with the beam energy losses demonstrates that only part of the missing beam energy is usually deposited as thermal excitation in the target nucleus. Requiring an additional coincidence with a light charged particle or fission fragment leads to selection of a significant higher average excitation energy. [S0556-2813(98)50408-6]

PACS number(s): 25.55.Ci, 25.70.Gh, 25.70.Jj, 27.80.+w

In recent experiments designed to study the high energy  $\gamma$  rays from the decay of the Giant dipole resonance (GDR) in  $^{208}\text{Pb}$  and  $^{120}\text{Sn}$  nuclei [1,2],  $\alpha$  particle inelastic scattering was used as a tool to populate low angular momentum states of stable nuclei at a moderate excitation energy (30–130 MeV). The observed GDR width increase was attributed to temperature effects, providing an important test of theoretical models [3,4]. In that work it was assumed that the energy loss (EL) in the collision could be used to tag the excitation energy ( $E_x$ ) of the target nucleus. Problems with this assumption can arise at intermediate energies when processes such as direct knockout and preequilibrium emission become important. In this case the excitation energy of the target fragment is lower than that corresponding to a complete transfer of the EL to the target nucleus as a whole. The importance of these processes can vary with the beam energy and scattering angle [5,6]. Thus, in order to employ such reactions in a systematic way to study the properties of excited nuclei, it is first necessary to experimentally determine the extent to which the energy loss of the inelastically scattered  $\alpha$  particles provides a good measure of the thermal excitation energy deposited in the target nucleus.

We present here results of experiments in which the excitation energy deposition in the reaction  $^{209}\text{Bi}(\alpha, \alpha')$  has been studied. We find that the average excitation energy deposition is well below the available energy. The selection of charged particle emission or fission channels serves to isolate nuclei of much higher excitation energy with narrower distribution widths. Coincident high energy  $\gamma$ -ray detection, as in Refs. [1,2], may provide a comparable selection of events but our results indicate that detailed information on the actual excitation energy distribution is required to study temperature induced effects in nuclei.

The experiments were carried out using the K500 Superconducting Cyclotron of the Texas A&M University Cyclotron Institute. A 4.5 mg/cm<sup>2</sup>  $^{209}\text{Bi}$  target was bombarded by a 240 MeV beam of  $\alpha$  particles. Emitted charged particles, neutrons, fission fragments, and low energy  $\gamma$  rays were detected in coincidence with the inelastically scattered  $\alpha$  particles. To this end several detectors were mounted inside the neutron ball (NB) calorimeter [7]. In the present experiment the NB wedge along the beam axis ( $\Delta\theta \pm 22.5^\circ$ ) in the forward hemisphere was replaced by a scattering chamber extension.

Inelastically scattered  $\alpha$  particles have been identified in a hodoscope, made of four large area  $\Delta E$ - $E$  telescopes placed around the beam axis at  $\langle\theta\rangle = 9^\circ$  (covering  $\Delta\theta \sim 11^\circ$ ). The  $\Delta E$  counter was a  $6 \times 4$  cm<sup>2</sup> silicon detector 300  $\mu\text{m}$  thick; the  $E$  detector was a CsI(Tl) scintillator, 3 cm thick, with photomultiplier readout. Light charged particles (LCP) and fission fragments (FF) have been detected in an additional six large area  $\Delta E$ - $E$  telescopes. Two of them were mounted at forward angles ( $\langle\theta\rangle = 37^\circ, -42^\circ, \phi = 0^\circ$ ) and four at backward angles ( $\langle\theta\rangle = -123^\circ, \phi = -49^\circ, 52^\circ$  and  $\langle\theta\rangle = 132^\circ, \phi = -49^\circ, 52^\circ$ ). Two germanium detectors (HPGe 80% relative efficiency) were also placed at  $100^\circ$  and  $140^\circ$  inside the NB to identify residual nuclei by discrete  $\gamma$ -line spectroscopy.

The master trigger of the experiment was the coincidence between the “fast flash” of the NB (indicating a reaction with prompt neutron and  $\gamma$  emission) and an  $\alpha$  particle in the hodoscope. The beam intensity was maintained around  $I = 0.01$  nA during the experiment to keep the trigger rate around 1 kHz.

The silicon detectors were calibrated with radioactive  $\alpha$  sources. The CsI(Tl) scintillator calibration was obtained from the calibrated  $\Delta E$  silicon, employing the energy loss tables, and from the measurement of  $\alpha$ , protons and deuterons elastic scattering at energies  $E_\alpha = 100$  MeV,  $E_p = 60$  MeV, and  $E_d = 120$  MeV, respectively.

The efficiency of the NB was determined using in-beam data from the HPGe detectors. Neutron fold distributions were obtained in coincidence with discrete  $\gamma$ -ray transitions identifying  $^{209,208,207}\text{Bi}$  nuclei populated after emission of 0,

\*Permanent address: Department of Physics, Hope College, Holland, MI 49423.

†Permanent address: Institute of Physics, Jagellonian University, 30-059 Cracow, Poland.

‡Permanent address: Instituto de Fisica, UNAM AP-20 364, Mexico City, 0100 DF, Mexico.

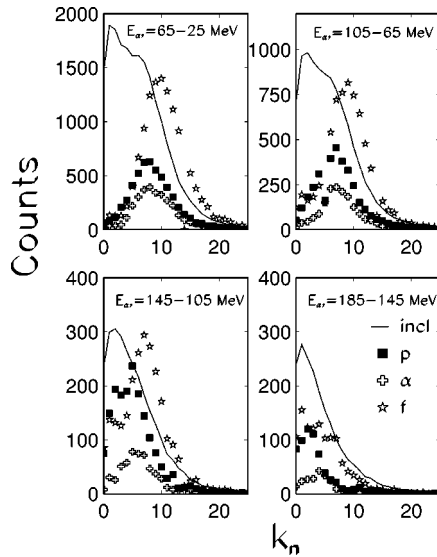


FIG. 1. Neutron fold distribution measured in the neutron ball for selected bins of the scattered  $\alpha$  particle energy  $E_{\alpha'}$ . Distributions corresponding to different event selections are reported: inclusive (line), coincidences with backward emitted protons (square),  $\alpha$  particles (cross), and fission fragments (star). Counts in the inclusive distributions are divided by factors of 10–20.

1, or 2 neutrons. The first moments of the fold distributions were used to determine the NB efficiency value of  $70 \pm 3\%$ . This value is consistent with the efficiency of 75% measured using a  $^{252}\text{Cf}$  source.

Experimental distributions of the neutron fold  $k_n$  from the NB are shown in Fig. 1 for some selected bins in the energy of the scattered  $\alpha$  particle ( $E_{\alpha'}$ ). The distributions at a given energy loss for inclusive events (coincidences between  $\alpha'$  and neutrons in the NB) are very broad, much more than expected from the binning in  $E_{\alpha'}$ . They include low  $k_n$  events, characteristic of low excitation energy, as well as events of higher  $k_n$ , where larger excitation energies are presumed. Note that these distributions are not background corrected. Average neutron multiplicities presented in the following are corrected for average multiplicities in the background gate of the NB. Figure 1 also shows  $k_n$  distributions obtained for exclusive events by requiring an additional coincidence with an LCP or a FF, detected in a backward telescope. This triple coincidence requirement should magnify the thermal emission with respect to the concurrent nonequilibrium emission. An inspection of the LCP energy spectra in both backward and forward telescopes, as well as their correlation plots with the neutron fold (not reported here), confirm this assumption. These spectra exhibit barriers characteristic of emission from Bi-like nuclei and have shapes which indicate a dominance of statistical emission.

In Fig. 2 the dependence of the average neutron multiplicities  $\langle \nu \rangle$ , obtained from the background and efficiency corrected NB fold distributions for inclusive and exclusive events, are presented as a function of  $E_{\alpha'}$ . The inclusive data show the expected positive correlation between energy loss and average neutron multiplicity. The latter saturates around the value  $\langle \nu \rangle \sim 7$  for  $\text{EL} \sim 200$  MeV. This average number of emitted neutrons is less than expected, as demonstrated by a comparison with the corresponding quantity in the fusion-evaporation reaction  $^{11}\text{B} + ^{198}\text{Pt} \rightarrow ^{209}\text{Bi}^* [8]$ . In

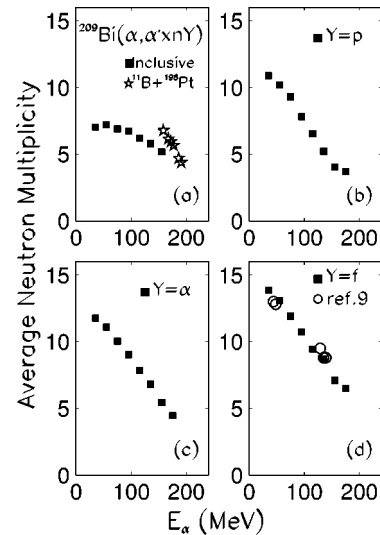


FIG. 2. Average neutron multiplicity as measured with the neutron ball (efficiency and background corrected) as a function of the energy of the scattered  $\alpha$  particles. Data corresponding to different event selections are reported: inclusive (a), coincidences with backward emitted protons (b),  $\alpha$  particles (c), and fission fragments (d). Data from fusion-fission [9] and fusion-evaporation reactions [8] are also reported, assuming the equivalence between the excitation energy in fusion and the kinetic energy loss in the  $\alpha$  scattering.

this case, where the excitation energy of the compound system is rather well determined, seven neutrons are emitted, on average, at  $E_x = 82$  MeV. These results indicate that the measure of the apparent energy loss in the scattering of  $\alpha$  particles on a heavy target cannot be taken directly as a measure of the target excitation energy which seems to be, on average, much lower.

The data for the exclusive events feature larger  $\langle \nu \rangle$  than the inclusive one, when the same EL is considered. The fission data allow a further interesting comparison with results from heavy ion induced reaction studies in which the average total neutron multiplicity accompanying fission has been measured for nuclei in the mass region  $A \sim 200$  [9]. The very good agreement between the two data sets demonstrates that the fission fragment requirement selects events in which nearly the entire kinetic energy loss observed in the scattering reaction is converted into thermal excitation energy of the target nucleus.

Finally, the correlation between the excitation energy in the target nucleus and the kinetic energy loss in the  $(\alpha, \alpha')$  reaction has been quantitatively studied. For each  $E_{\alpha'}$  bin, the total excitation energy transferred to the target nucleus has been derived by determining the energy dissipated in the emission of the detected decay products. As an example of this procedure, we describe here the case for the proton trigger in the backward detectors at  $\text{EL} = 205$  MeV, for which  $\langle \nu \rangle = 10.9$  is measured. We evaluate the total  $Q$  value for the decay  $^{209}\text{Bi} \rightarrow ^{197}\text{Pb}$ ,  $Q = 87.3$  MeV from mass tables [10]. Then we derive an average center-of-mass kinetic energy  $\langle \epsilon_p \rangle = 13.1$  MeV from the experimental proton spectrum and  $\langle \epsilon_n \rangle = 3.5$  MeV for the evaporated neutrons using statistical model calculations. This gives a total kinetic energy of 51.2 MeV dissipated in the particle emission. An additional term (8 MeV) accounts for the gamma decay at the end of the

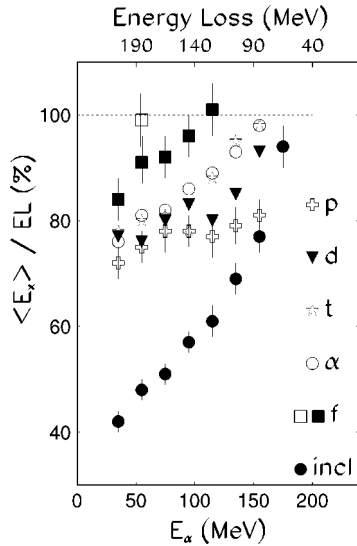


FIG. 3. Ratio between the reconstructed excitation energy of the targetlike fragment and the corresponding energy loss determined from the energy of the scattered  $\alpha$  particles. The error bars include only the uncertainty in the efficiency calibration of the neutron ball calorimeter. The open square point for the fission events ( $f$ ) includes a correction for the emission of charged particles. For details see the text.

evaporative process. The total energy dissipated in the decay is therefore  $\sim 146$  MeV, which represents  $\sim 72\%$  of the corresponding  $\alpha$ -particle kinetic energy lost in the  $(\alpha, \alpha')$  reaction.

As  $E_{\alpha'}$  decreases from 150 to 35 MeV, the reconstructed average excitation energies increase ranging between 68 and 146 MeV for protons or between 83 and 157 MeV for  $\alpha$  particles and heavy hydrogen isotopes. The missing energy is because of the emission of undetected particles mainly in nonequilibrium processes. (Note that the NB calorimeter exhibits a reduced efficiency for energetic neutrons emitted in the forward direction because of the dependence of the intrinsic efficiency on the neutron energy [7] as well as to the reduced coverage. Using the observed preequilibrium proton yields, angular distributions, and energies, we estimate a contribution  $\leq 0.2$  fold unit from the detection of preequilibrium neutrons.)

The ratios of the reconstructed average excitation energies  $\langle E_x \rangle$  to the nominal total kinetic energy losses EL for the different class of events are shown in Fig. 3, as a function of  $E_{\alpha'}$ . Even though the deposited excitation energy is increasing in absolute value, a constant decrease of the ratio  $\langle E_x \rangle / EL$  is evident as  $E_{\alpha'}$  decreases. The clear difference in the excitation energy selection for the clusters ( $\alpha, t$ ) and protons reflects, in our opinion, the fact that particles characterized by a large binding energy ( $t$ ) or barrier ( $\alpha$ ) need a larger excitation energy to be emitted with significant probability. This means that for a given energy loss the “energetically expensive” particles originate, on average, from those target nuclei that receive the larger fraction of the available energy.

The data corresponding to the coincidences with fission fragments are also shown in Fig. 3. In this case the reconstruction of the excitation energy is more involved because of the complexity of the decay scheme and the need to include the fission fragment total kinetic energy (TKE). A par-

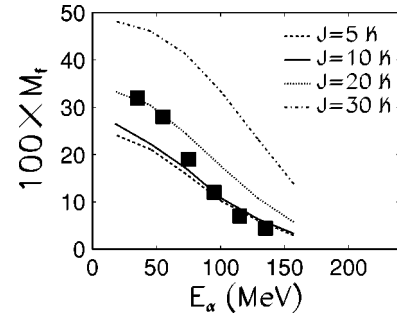


FIG. 4. Experimental fission multiplicity  $M_f$  compared with PACE2 statistical model calculations. For details see the text.

titution of  $\langle \nu \rangle$  between the pre- ( $\langle \nu_{\text{pre}} \rangle$ ) and the postscission ( $\langle \nu_{\text{post}} \rangle$ ) stage was assumed following Ref. [9]. The energy dissipated in pre-scission decay is evaluated as described above for the LCP events. Then the fission  $Q$  value is estimated as

$$Q_{ff} = M(A_{CN'}, 83) - [M(A_{CN'}/2, 41) + M(A_{CN'}/2, 42) + \text{TKE}],$$

where  $A_{CN'} = 209 - \langle \nu_{\text{pre}} \rangle$  is the assumed mass of the fissioning nucleus and the TKE value was taken from Ref. [11]. In the postscission stage, the decaying fission fragments are assumed to emit the remaining neutrons  $\langle \nu_{\text{post}} \rangle$  and their excitation energy dissipation is also estimated accordingly.

The results for the fission trigger in Fig. 3 feature a  $\langle E_x \rangle / EL$  ratio of about 90%. The missing energy at the larger energy losses seems in this case to be due to the charged particles emitted in both the pre- and postscission stages. This is estimated from our data and statistical model calculations to be  $\Delta E_x \sim 16$  MeV. Taking into account this correction, the  $\langle E_x \rangle / EL$  ratio moves very close to unity as indicated by the open square in the figure.

The experimental fission multiplicity is shown in Fig. 4, compared with results from statistical model calculations performed with the code PACE2 [12] for the  $^{209}\text{Bi}$  nucleus at different excitation energies ( $E_x^{\text{PACE2}}$ ) and single angular momentum values ( $J$ ). In the calculations, the level density parameters  $a_v = a_f = A/10 \text{ MeV}^{-1}$  were used, in the evaporation and fission channels, together with the Sierk fission barriers [13]. The model predictions have been reported in Fig. 4 by assuming a ratio  $E_x^{\text{PACE2}} / EL = 0.9$ . The comparison shows that the experimental data are well described by calculations employing angular momentum values  $J \leq 20\hbar$  up to the highest energy losses. We note that, because of the strong dependence of the fission cross section on the angular momentum, coincidences with fission fragments are certainly sampling the events in which the highest angular momenta are transferred to the target nucleus.

The results reported here demonstrate that the excitation energy deposition in inelastic scattering of  $\alpha$  particles at 60 MeV/nucleon is, on average, well below the projectile kinetic energy loss. From the fold distribution of the neutron ball it appears that the distribution of excitation energies in targetlike nuclei includes nuclei at high excitation energy but is very broad.

A threshold in the detected number of neutrons can be used to isolate the high excitation energy events, although the finite response of the calorimeter does not allow precise tagging of the excitation energy event by event. As an alternative possibility, high excitation energy nuclei can be filtered out by requiring coincidences with LCP or fission fragments. The efficiency of the filter is related to the excitation energy dependence of the multiplicity of the different decay products.

This filtering effect may also be effective in the case of the high energy  $\gamma$  rays of Refs. [1,2], as the probability of GDR excitation is expected to increase over the excitation energy range studied. However the precise determination of the excitation energy selected by  $\alpha$ -high energy  $\gamma$ -rays coincidences requires more complete information. Furthermore the line shapes of the  $\gamma$  spectra measured in coincidence with the scattered alpha particles should be influenced by the width of the selected excitation energy range since the statistical part of the  $\gamma$  spectrum is emitted also from nuclei at low excitation energy while the high energy part, in the GDR region, originates mainly from the higher excitation energy

region. Without taking the width of the excitation energy distribution explicitly into account, the line shape analysis might lead to extraction of erroneous GDR parameters [14].

We are currently exploiting the possibility of reconstructing the excitation energy distribution in primary targetlike nuclei by unfolding the experimental  $k_n$  spectra and using statistical model predictions. This will allow us to study in a more quantitative way the effects of the excitation energy distribution on the high energy  $\gamma$ -ray spectra.

The systematic use of inelastic  $\alpha$  particle scattering to produce nuclei with excitation energies  $E_x = 100\text{--}200$  MeV seems to be conditioned on the possibility of specifying in a more precise way the excitation energy of the targetlike fragments. Further progress is also needed in the theoretical treatments. Having calculations capable of describing not only the shapes of the scattered  $\alpha$  particle spectra [15] but also the transfer of excitation energy and angular momentum to the target nucleus would be extremely beneficial.

This work was supported by the U.S. Department of Energy, the Robert A. Welch Foundation, and the INFN.

- 
- [1] E. Ramakrishnan *et al.*, Phys. Lett. B **383**, 252 (1996).  
 [2] E. Ramakrishnan *et al.*, Phys. Rev. Lett. **76**, 2025 (1996).  
 [3] V. Baran *et al.*, Nucl. Phys. **A599**, 29c (1996).  
 [4] W. E Ormand, P. F. Bortignon, and R. A. Broglia, Phys. Rev. Lett. **77**, 607 (1996).  
 [5] H. Ejiri, J. Phys. C **45**, 135 (1984).  
 [6] See, E. Gadioli and P. E. Hodgson, *Pre-equilibrium Nuclear Reactions* (Oxford Science, Oxford, England, 1992).  
 [7] R. P. Schmitt *et al.*, Nucl. Instrum. Methods Phys. Res. A **354**, 487 (1995).  
 [8] D. Fabris *et al.*, J. Phys. G **23**, 1377 (1997); M. Lunardon, Ph.D. Thesis, University of Padova, 1998.  
 [9] D. J. Hinde *et al.*, Phys. Rev. C **45**, 1229 (1992).  
 [10] G. Audi and A. H. Wapstra, Nucl. Phys. **A565**, 1 (1993).  
 [11] V. Viola, Phys. Rev. C **31**, 1550 (1985).  
 [12] See A. Gavron, Phys. Rev. C **21**, 230 (1980).  
 [13] A. J. Sierk, Phys. Rev. C **33**, 2039 (1986).  
 [14] M. P. Kelly *et al.*, Phys. Rev. C **56**, 3201 (1997).  
 [15] M. B. Chadwick *et al.*, Acta Phys. Hung. New Ser.: Heavy Ion Phys. **2**, 347 (1995).